ELECTRON TRANSPORT THROUGH EXPERIMENTALLY CONTROLLABLE PARABOLIC BUBBLES ON GRAPHENE NANORIBBONS

MAI-CHUNG NGUYEN[1,2,*], HUY-VIET NGUYEN[3,†]

[1]*Graduate University of Science and Technology, Vietnam Academy of Science and Technology, 18 Hoang Quoc Viet, Cau Giay, Hanoi, Vietnam*

[2]*Energy Department, University of Science and Technology of Hanoi, Vietnam Academy of Science and Technology, 18 Hoang Quoc Viet, Cau Giay, Hanoi, Vietnam*

[3]*Institute of Physics, Vietnam Academy of Science and Technology, 18 Hoang Quoc Viet, Cau Giay, Hanoi, Vietnam*

E-mail: *nguyen-mai.chung@usth.edu.vn; †nhviet@iop.vast.vn

Abstract. *We present a theoretical study of electron transport properties through experimentally controllable graphene nanobubbles [P. Jia et al., Nat. Commun. **10** (2019) 1] employing a tight-binding model and the non-equilibrium Green's function formalism. Sharp conductance peaks are observed at low energy region which signifies the emergence of quasi-bound states caused by pseudomagnetic field in the strained nanobubbles. Analysis based on local density of states reveals the nature of electron transmission at peak energies. Our results also show that the emergence of quasi-bound states and its role in electron transport depend on both strain strength and bubble size: when the strain or size of the bubble increases, more quasi-bound states emerge and resonant tunnelling assisted by these quasi-bound states becomes dominant.*

I. INTRODUCTION

Thanks to its excellent electronic properties, graphene is a promising candidate for electronic technology innovation. However, practical applications of 2D graphene in conventional semiconductor devices are still challenging due to its gapless nature [1, 2]. Strain engineering has been proven to be effective in tuning electronic properties of graphene as well as other 2D

materials [3–5]. Under a strain, C–C bond lengths in graphene change which alters the magnitude of hoping energies of π-electrons between carbon atoms. This effects electron dynamics in a very similar way to applying an external magnetic field. While a real magnetic field acts similarly on electrons at K and K' Dirac points, effect of a strain is as if electrons at K and K' feel opposite magnetic fields, thus often referred to as pseudo-magnetic field (PMF). Following a theoretical prediction of a zero-field quantum Hall effect in a designed triaxial strain [6], an experiment observation of Landau levels in highly-strained graphene nanobubbles (GNB) was reported [7]. Since then, graphene nanobubbles–local, out-of-plane deformations on graphene sheets–has been a subject of much interest for both experimental and theoretical studies thanks to its large PMFs, up to several hundreds Tesla, that is not possible to achieve with magnets in laboratory.

From an experimental standpoint, the formation of bubbles due to trapped gas or liquid is almost inevitable when a graphene sheet is transferred to a substrate. On one hand, this is certainly unwanted because it causes a degradation of many excellent electrical properties of graphene. On the other hand, it can serve as a way to strain engineer graphene for potential applications if the formation of the bubbles can be put under a controlled manner. In fact, it has been reported recently that programmable GNBs, i.e. the creation of bubbles with expected location and size/shape, are possible using atomic force microscope [8]. In short, the bubble is formed when hydrogen atoms in hydrogen-terminated graphene, which is grown on a clean Ge(110) surface by chemical vapor deposition, desorb and evolve into hydrogen molecules when a negative stimulus voltage is applied to the tip. The precision of AFM tip allows one to a create bubble at the pre-defined location while the contour profile of the bubble can be changed by tuning the tip voltage. When the tip voltage is small, the entire bubble has a parabolic profile. For larger voltages, while the bottom of the bubble is still parabolic, the top region changes to a Gaussian profile.

Theoretical investigations of electron transport in graphene nanobubbles mainly focused on Gaussian-shaped deformations whose strain-induced PMF can be calculated analytically [9, 10]. The main result is that the stronger the deformation is, the larger the reduction in electron conductance was observed. This is considered as a signature of electron confinement caused by the bubbles. However, bubbles considered in these studies are rather small, with the radii of about 5 nm at the maximum. Such small bubbles are randomly formed, thus it is difficult to control their size and location for practical applications. In this paper, we report our investigation of transport properties of electrons in experimentally controllable parabolic-shaped nanobubbles with base radii up to 50 nm [8]. The appearance of conductance peaks at low energy region signifies the emergence of quasi-bound states in the bubbles and can be understood by the resonance with continuum states in the infinite leads. The rest of the paper is organized as follows. In Section II, a tight-binding model that takes into account the effect of strain is introduced to describe electrons in nanobubbles. The model is then solved by employing recursive technique within the non-equilibrium Green's function formalism. Numerical results for conductance together with detailed analyses based on local density of states (LDoS) will be presented in Section III. Our conclusions and outlook are in the last Section.

II. **MODELS AND CALCULATION METHODOLOGY**

In this study, graphene nanobubbles as experimentally fabricated in a controlled manner in Ref. [8] are modeled by out-of-plane, parabolic-shaped deformations on an armchair graphene nanoribbon as schematized in the Fig. 1. The shape of the parabolic bubble is uniquely determined
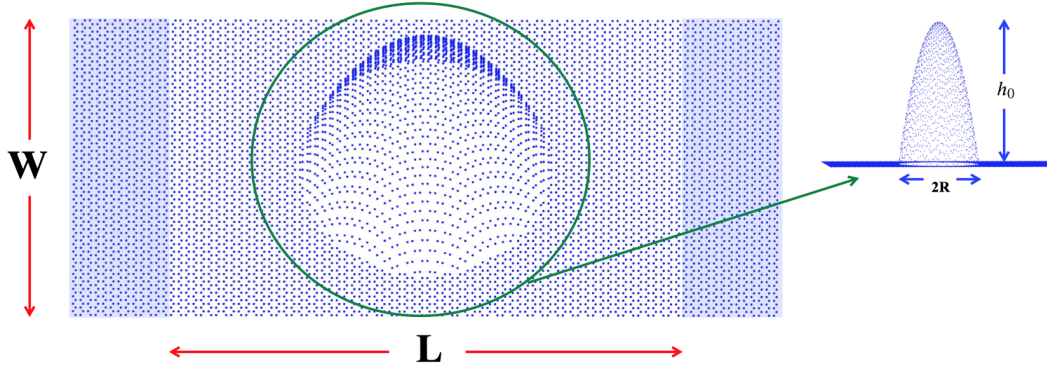
Fig. 1. Schematic of deformed parabolic-shaped bubble studied in this work. Deformation is applied locally in the central region of an armchair graphene nanoribbon with the width W and the length L which is connected to two semi-infinite leads. Two parameters, i.e. the maximum height h_0 and the radius of the base R, that define a bubble are shown on the right.

by two parameters h_0 (the maximum height) and R (the base radius) which are also illustrated in the right of Fig. 1. The height of carbon atoms in the centrosymmetrically-deformed parabola is given by

$$h(x,y) = h_0(1 - \frac{(x-x_0)^2 + (y-y_0)^2}{R^2}),$$ (1)

where x_0, y_0 are the coordinates of carbon atoms at the centre of the bubble. For simplicity, in-plane displacements are neglected, thus (x,y) coordinates of carbon atoms in undeformed ribbon were used to calculate out-of-plane displacements in the above equation. For given bubble, the width, i.e. the dimension along the zigzag direction, of the ribbons is chosen to be 1.5 times larger than the diameter of the base of the bubbles. This is large enough to remove effects of the boundaries on the bubbles since the base diameter of the smallest bubble reported in the experiment is already 50 nm and the deformation vanishes beyond the distance larger than the radius. The length, i.e. the dimension along the armchair direction, of the nanoribbons is however larger than the width about 25% because this is the transport direction in the non-equilibrium Green's functions (NEGF) formalism employed in the calculation of electronic quantities such as density of states (DoS), local DoS, transmission functions.

An atomistic tight-binding model was used to describe the electronic properties of the structure. The Hamiltonian reads

$$H_{tb} = \sum_n U_n c_n^\dagger c_n + \sum_{nm} t_{nm} c_n^\dagger c_m,$$ (2)

where U_n is the potential energy at the nth site and t_{nm} is the hopping energy between nearest neighbor n^{th} and m^{th} sites. Under the strain introduced by the parabola-shaped deformation, the C–C bond vectors are changed as shown in Ref. [11]. The hopping parameter between atoms is determined by [12]

$$t_{nm} = t_0 \exp[-3.37(r_{nm}/r_0 - 1)]$$ (3)

with $t_0 = -2.8$ eV and $r_0 = 0.142$ nm being the hopping energy and the C-C distance in unstrained graphene, respectively. r_{nm} is the distance between the nth and m^{th} atoms and is calculated as $r_{nm} = \sqrt{(x_n - x_m)^2 + (y_n - y_m)^2 + (z_n - z_m)^2)}$.

As in Refs.- [13,14], we employed the non-equilibrium Green's function formalism within the ballistic approximation to investigate the electronic transport properties of the devices. The Green's function is then computed using the equation [15]:

$$G = [\epsilon + i0^+ - H_{tb} - \Sigma_L - \Sigma_R]^{-1}, \qquad (4)$$

with $\Sigma_{L(R)}$ being the self-energies that describe the left (right) contact-to-device couplings which can be calculated analytically for an AGNR [16]. The transmission probability is calculated as $T_e = \text{Tr}\{\Gamma_L G \Gamma_R G^\dagger\}$, with $\Gamma_{L(R)} = i(\Sigma_{L(R)} - \Sigma_{L(R)}^\dagger)$ being the transfer rate at the left (right) contact. Direct inversion of matrices to obtain the Green's function is computationally intractable due to very large matrices involved. To overcome this problem, we employed recursive algorithms for evaluating G that allow us to deal with systems containing up to a million of atoms [15–17]. Once the Green's function is obtained, the local density of states (LDoS) at the nth lattice site is computed as

$$D(\vec{r}_n, E) = -\frac{\text{Im}[G_{nn}(E)]}{\pi} \qquad (5)$$

III. RESULTS AND DISCUSSION

It is well-known that AGNRs can be metallic ($2M = 3p+2$) or semiconducting ($2M = 3p$ or $3p+1$), depending on the number of carbon dimers, M, along the width. Thus, we will investigate the effect of parabolic deformation on the electronic properties for all three cases. The width of an AGNR is given by $W = M \times \sqrt{3} \times a_0$, where $a_0 = 1.42$ Å is the distance between two neighboring atoms in pristine graphene. For the sake of brevity, we will denote nanoribbons as $3p0$–, $3p1$–, and $3p2$–ribbon, respectively. We start with the smallest bubble reported in Ref. [8] with the radius $R = 30$ nm and the height $h_0 = 2.5$ nm. Even for this smallest bubble, the required nanoribbons in our calculation are rather large which are rectangles of dimensions 120×90 nm and contain more than 400 000 atoms. Throughout this work, the bubble is located at the center of the ribbon.

Fig. 2 shows the conductance and DoS as a function of Fermi energy for three cases with $M = 366, 365$ and 364. We note that spin degeneracy is assumed which explains for the factor of 2 in the unit of conductance axes. Compared to perfect nanoribbons, the conductance is reduced when the bubbles are present as one can see clearly in the top panel (red solid lines versus blue dashed ones). This is not surprising because deformations introduce pseudo-magnetic potentials which act as scattering regions, causing a degradation in transport of electrons. This is also consistent with the DoS pictures in Fig. 2(d,e,f). However, a striking feature is clearly observed in the DoS, namely the presence of sharp peaks, especially at low energy region, for all three cases when the deformation is turned on (red solid line in the bottom panel). To inspect the effect of these peaks on electron transport properties, we look into the conductance at a smaller energy scale as displayed in the insets of three figures of the top panel. For each case, two sharp resonant peaks are present in the conductance graph. Surprisingly, some resonant peaks appear even in the gapped region for the case of semiconducting ribbons. This is a strong indication of the formation of quasi-bound states in the bubbles. We note that the role of quasi-bound states in resonant

transport through pseudo-magnetic quantum dots created by in-plane, triaxial strain [18] as well as magnetic quantum dots in the quantum Hall regime [19] was proposed before.
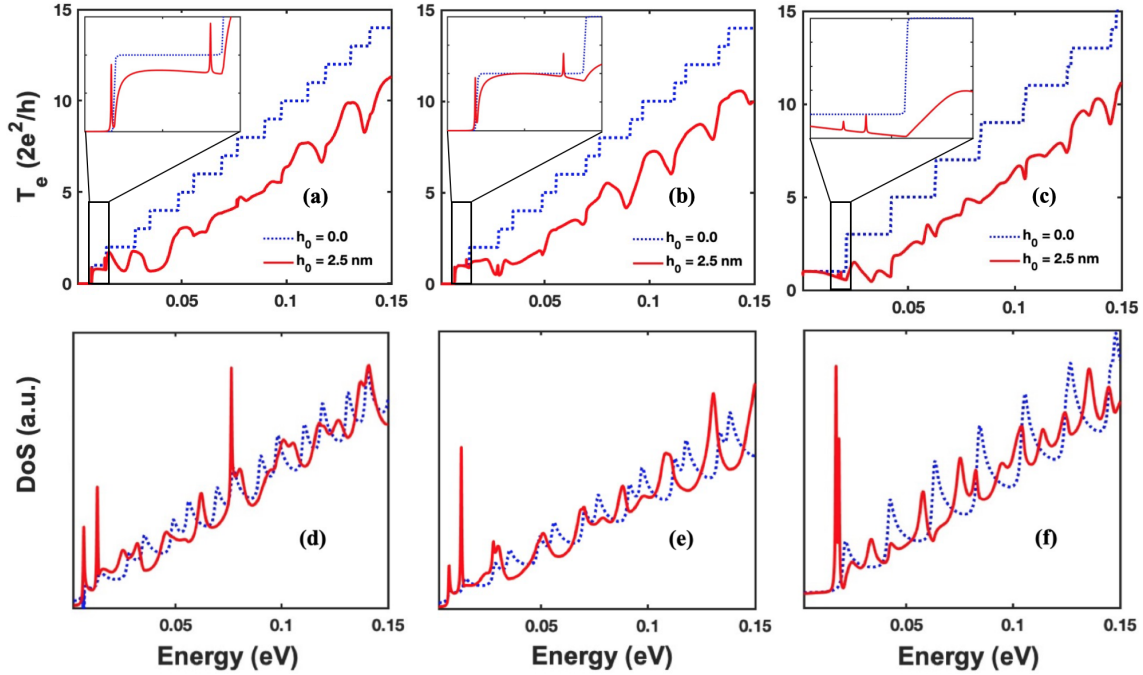

Fig. 2. (color online) Conductance (solid red line, upper panel) and DoS (solid red line, lower panel) as a function of Fermi energy for the parabolic bubble with radius $R = 30$ nm and height $h_0 = 2.5$ nm located at the center of semiconducting (a,d)($M = 366$) and (b,e)($M = 365$), and metallic (c,f)($M = 364$) 120×90 nm rectangular AGNRs. For comparison, the same quantities undeformed AGNRs are also drawn in dashed blue lines.

To understand the nature of the observed resonant transport, we examine LDoS at peak energies which are shown in Fig. 3 by contour plots (LDoS is zero in the white region). Two distinct features are observed for three cases. First, LDoS at energies corresponding to both peaks of $3p0-$ and the first peak of $3p1-$ribbons spread to both left and right leads despite of still being more concentrated in the bubbles. We note that these peaks are quite close to the energy windows where the next subband start to play a dominant role in electron transport. This can be seen in the insets of the top panel in Fig. 2, namely the rapid increase of conductance right after the peak energies. Thus one can attribute this feature to some kind of mixing between these quasi-bound states and the extended Bloch's states in undeformed nanoribbons. Three other cases, i.e. LDoS at energies corresponding to the second peak of $3p1-$ and both peaks of $3p2-$ribbons show well-localized electronic wavefunctions, especially from two leads. This indicates that these quasi-bound states are weakly coupled to the leads and thus the resonant tunnelling mechanism play a dominant role.
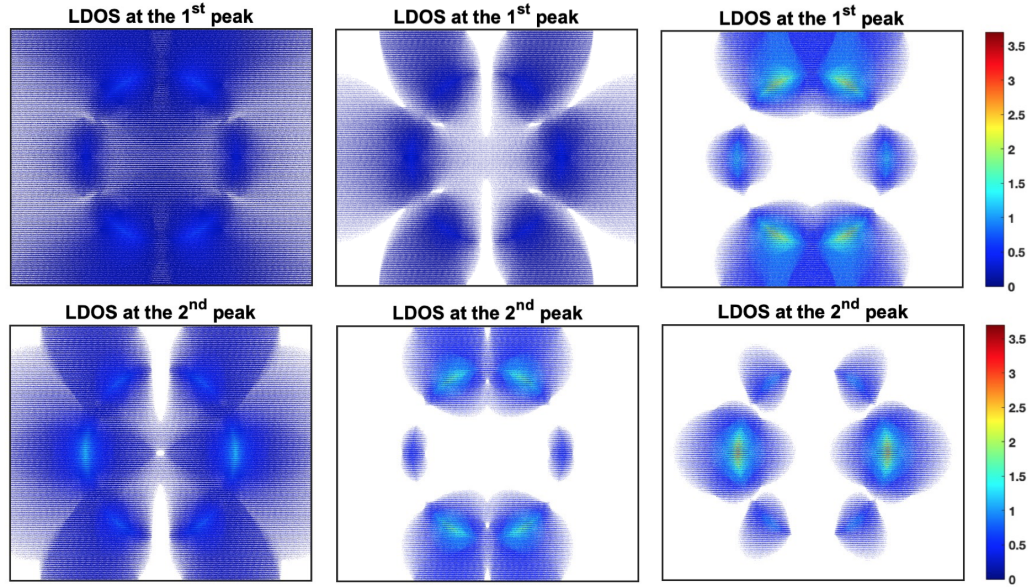
Fig. 3. Contour plots of LDoS at energies corresponding to the first and second peaks of conductance shown in the insets of Fig. 2.
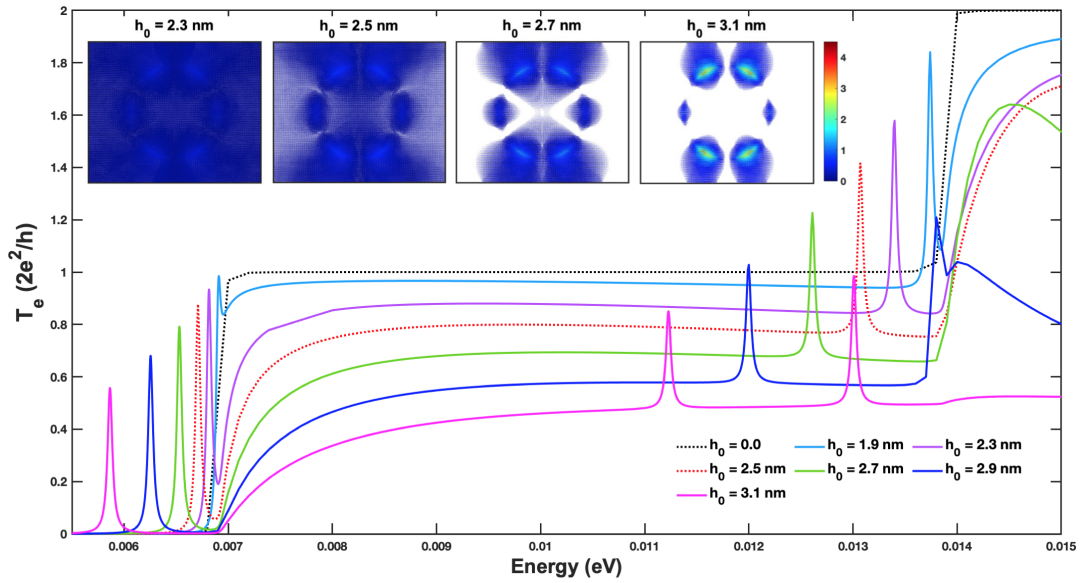
Fig. 4. (color online) Conductance as a function of Fermi energy for parabolic bubbles with fixed radius $R = 30$ nm and bubble height, h_0, varying around the experimental value of 2.5 nm (red dotted line). The insets are LDoS at energies corresponding to the first peaks for selected values of h_0 which show a stronger confinement as h_0 increases.

Next, we investigate the effect of strain strength on quasi-bound states by varying the height of the nanobubble around the experimental values $h_0 = 2.5$ nm, while keeping the base radius $R = 30$ nm unchanged. We note that maximum strain defined as the ratio of the largest C-C bond length in deformed ribbon and the undeformed one for this case is about 1.4% which is still very small compared to the largest strain that a graphene sheet can endure [20]. Fig. 4 shows the conductance for different bubble heights of the representative case of $3p0-$ribbon. The general trend is that when the bubble height increases, the resonant peaks shift to lower energies, together with a decrease in the peak heights. This can be understood as follows. As one can expect, the larger the maximum height h_0, the greater the strain strength in the bubble (2.1% for the case of $h_0 = 3.1$ nm) which causes a stronger pseudo-magnetic field. As a consequence, the confinement of electrons in the quasi-bound states increases as supported by the pictures of more localized LDoS of the first peaks shown in the inset of Fig. 4. This results in the smaller couplings with two leads, thus smaller peak heights when the transport is dominant by the tunnelling mechanism. It is also seen that the first conductance peak almost disappears for the case of $h = 1.9$ nm (strain of 0.8%). This indicates that quasi-bound states will not emerge when the strain is small.
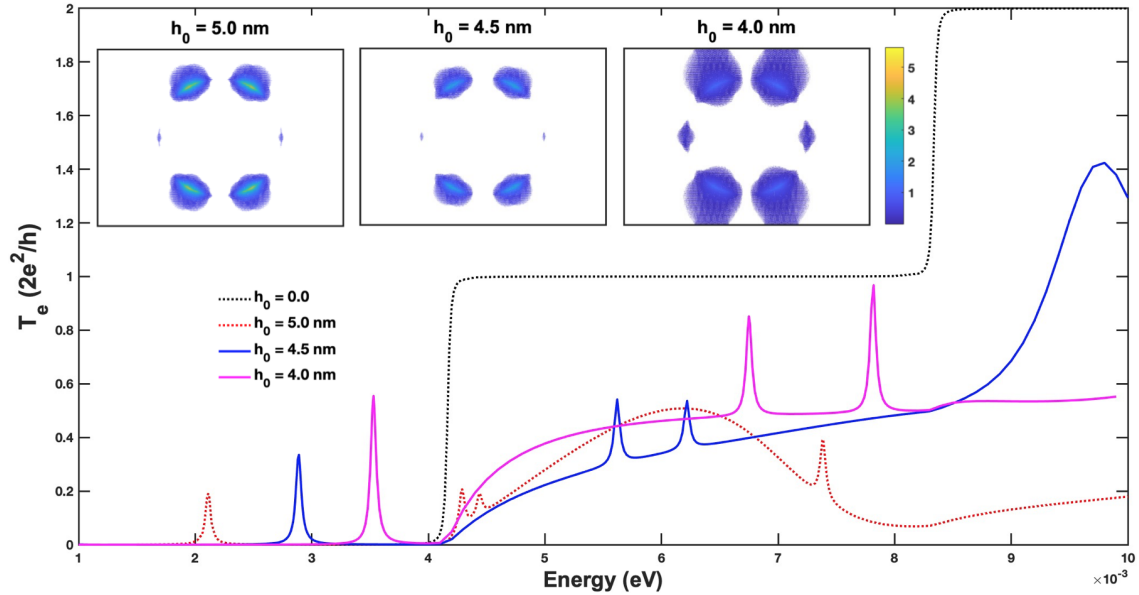
Fig. 5. Conductance as a function of Fermi energy for three parabolic bubbles having the same radius $R = 50$ nm, but different heights. The red, dotted line corresponds to $h_0 = 5.0$ which is the experimental value. The insets are LDoS at energies corresponding to the first peaks which also show a stronger confinement as h_0 increases.

Finally, we present the results for bubbles with larger radius of 50 nm in Fig. 5 where the conductance as a function of Fermi energy for several bubble heights were plotted. For comparison purposes, we chose to present the results for the representative case of $3p0-$ribbon with the width ~ 150 nm and the length ~ 200 nm which contains more than one million atoms. For the case of $h_0 = 5.0$ nm which was observed in experiment [8], resonant peaks are observed as before (see the red dotted line), but the number of peaks as well as their height and position are rather

different from that of the smaller bubble. Specifically, three peaks appear in the energy window corresponding to the first subband which is consistent with three peaks in the DoS picture (not shown) and the first resonant peak in the gapped region is also far from this energy window. This leads us to a speculation that this might be the behaviour corresponding to large strain region, despite of the fact that the maximum strain as defined before is about 2.0% for this case. To check this point, we also plotted in the same figure the conductance for two bubbles with smaller heights of 4.5 and 4.0 nm whose strain are 1.6% and 1.3%, respectively. It turns out that the observed resonant picture is qualitatively similar to what was obtained for smaller bubble with a strain of 2.1%, namely two resonant peaks in the energy window of the first subband. Well-localized LDoSs at the first peaks of three bubble heights as plotted in the insets of Fig. 5 show a strong confinement which further supports our speculation. These observation indicates that the emergence of quasi-bound states is also effected by the bubble size: quasi-bound states are easily formed and more localized in larger bubbles. Based on our observation here, we suspect that clear signatures of quasi-bound states were not observed and reported in previous studies [9, 10] because the Gaussian-shaped bubbles under study were too small, thus require much larger strain for quasi-bound states to emerge.

IV. CONCLUSIONS

In this work, we have investigated electron transport properties through nanobubbles formed on armchair graphene nanoribbons, focusing on the emergence of quasi-bound states and their role in electron transport. Unlike previous studies where rather small Gaussian-shaped bubbles with base radii less than 5 nm were used, we carried out tight-binding calculations within the non-equlibrium Green's function formalism for much larger parabolic-shaped bubbles which were realized in experiment with controllable precision of position and contour profile thanks to the utilization of atomic force microscopy techniques. For such a large bubble which contains up to million atoms, the calculations are only possible with efficient implementations of numerical algorithms, such as recursive Green's function and Haydock-Heine-Kelly recursive algorithm for evaluation of Green's function.

The emergence of quasi-bound states was observed in the conductance peaks and the localization properties of these states were analyzed using LDoS picture. Our results show that quasi-bound states emerge more easily in larger bubbles and they are more localized when strain is stronger. This localization determines the transport mechanism at the energies of quasi-bound states: resonant tunnelling plays a dominant role when the quasi-bound state is well localized from left and right leads. Although only parabolic-shaped bubbles were studied in this work, larger bubbles with Gaussian profile in the top region were also reported in experiment. We anticipate that more interesting transport properties could be observed for this mixed structure and this will be studied systematically, together with size effect discussed before and the role of ribbon types, in our future work.

REFERENCES

[1] K. S. Novoselov, A. K. Geim, S. V. Morozov, D.-e. Jiang, Y. Zhang, S. V. Dubonos et al., *Electric field effect in atomically thin carbon films*, Science **306** (2004) 666.

[2] A. C. Neto, F. Guinea, N. M. Peres, K. S. Novoselov and A. K. Geim, *The electronic properties of graphene*, Rev. Mod. Phys. **81** (2009) 109.

[3] V. M. Pereira and A. H. Castro Neto, *Strain engineering of graphene's electronic structure*, Phys. Rev. Lett. **103** (2009) 046801.

[4] C. Si, Z. Sun and F. Liu, *Strain engineering of graphene: a review*, Nanoscale **8** (2016) 3207.

[5] S. Yang, Y. Chen and C. Jiang, *Strain engineering of two-dimensional materials: Methods, properties, and applications*, InfoMat **3** (2021) 397.

[6] F. Guinea, M. Katsnelson and A. Geim, *Energy gaps and a zero-field quantum hall effect in graphene by strain engineering*, Nat. Phys. **6** (2010) 30.

[7] N. Levy, S. Burke, K. Meaker, M. Panlasigui, A. Zettl, F. Guinea et al., *Strain-induced pseudo–magnetic fields greater than 300 tesla in graphene nanobubbles*, Science **329** (2010) 544.

[8] P. Jia, W. Chen, J. Qiao, M. Zhang, X. Zheng, Z. Xue et al., *Programmable graphene nanobubbles with three-fold symmetric pseudo-magnetic fields*, Nat. Commun. **10** (2019) 1.

[9] R. Carrillo-Bastos, D. Faria, A. Latgé, F. Mireles and N. Sandler, *Gaussian deformations in graphene ribbons: Flowers and confinement*, Phys. Rev. B **90** (2014) 041411.

[10] V.-T. Tran, J. Saint-Martin and P. Dollfus, *Electron transport properties of graphene nanoribbons with gaussian deformation*, Phys. Rev. B **102** (2020) 075425.

[11] D. A. Bahamon and V. M. Pereira, *Conductance across strain junctions in graphene nanoribbons*, Phys. Rev. B **88** (2013) 195416.

[12] V. M. Pereira, A. H. Castro Neto and N. M. R. Peres, *Tight-binding approach to uniaxial strain in graphene*, Phys. Rev. B **80** (2009) 045401.

[13] M. C. Nguyen, V. H. Nguyen, H.-V. Nguyen and P. Dollfus, *Conduction gap in graphene strain junctions: direction dependence*, Semicond. Sci. Technol **29** (2014) 115024.

[14] M. C. Nguyen, V. H. Nguyen, H.-V. Nguyen, J. Saint-Martin and P. Dollfus, *Enhanced seebeck effect in graphene devices by strain and doping engineering*, Physica E **73** (2015) 207.

[15] M. Anantram, M. S. Lundstrom and D. E. Nikonov, *Modeling of nanoscale devices*, Proceedings of the IEEE **96** (2008) 1511.

[16] C. H. Lewenkopf and E. R. Mucciolo, *The recursive green's function method for graphene*, J. Comput. Electron. **12** (2013) 203.

[17] R. Haydock, V. Heine and M. Kelly, *Electronic structure based on the local atomic environment for tight-binding bands*, J. Phys. C: Solid State Phys. **5** (1972) 2845.

[18] Z. Qi, D. Bahamon, V. M. Pereira, H. S. Park, D. Campbell and A. C. Neto, *Resonant tunneling in graphene pseudomagnetic quantum dots*, Nano Lett. **13** (2013) 2692.

[19] N. Myoung, J.-W. Ryu, H. C. Park, S. J. Lee and S. Woo, *Splitting of conductance resonance through a magnetic quantum dot in graphene*, Phys. Rev. B **100** (2019) 045427.

[20] C. Lee, X. Wei, J. W. Kysar and J. Hone, *Measurement of the elastic properties and intrinsic strength of monolayer graphene*, Science **321** (2008) 385.